Spatiotemporal Modeling of Real World Backsheets Field Survey Data: Hierarchical (Multilevel) Generalized Additive Models

Preprint

Raymond J. Wieser,[1] Zelin (Zack) Li,[1] Stephanie L. Moffitt,[2] Ruben Zabalza,[3] Evan Boucher,[3] Silvana Ayala,[4] Matthew Brown,[4] Xiaohong Gu,[2] Liang Ji,[3] Colleen O'Brien,[3] Adam W. Hauser,[6] Greg S. O'Brien,[6] Xuanji Yu,[1] Roger H. French,[1] Micheal D. Kempe,[4] Jared Tracy,[5] Kausik R. Choudhury,[5] William J. Gambogi,[5] Laura S. Bruckman,[1] and Kenneth P. Boyce[3]

1 Case Western Reserve University
2 National Insitute of Standards and Technology
3 Underwriter Laboratories
4 National Renewable Energy Laboratory
5 DuPont Photovoltaic Solutions
6 Arkema, King of Prussia

Presented at the 49th IEEE Photovoltaic Specialists Conference (PVSC 49)
Philadelphia, Pennsylvania
June 5-10, 2022

NREL is a national laboratory of the U.S. Department of Energy
Office of Energy Efficiency & Renewable Energy
Operated by the Alliance for Sustainable Energy, LLC

Conference Paper
NREL/CP-5K00-81961
September 2022

This report is available at no cost from the National Renewable Energy Laboratory (NREL) at www.nrel.gov/publications.

Contract No. DE-AC36-08GO28308

Spatiotemporal Modeling of Real World Backsheets Field Survey Data: Hierarchical (Multilevel) Generalized Additive Models

Preprint

Raymond J. Wieser,[1] Zelin (Zack) Li,[1] Stephanie L. Moffitt,[2] Ruben Zabalza,[3] Evan Boucher,[3] Silvana Ayala,[4] Matthew Brown,[4] Xiaohong Gu,[2] Liang Ji,[3] Colleen O'Brien,[3] Adam W. Hauser,[6] Greg S. O'Brien,[6] Xuanji Yu,[1] Roger H. French,[1] Micheal D. Kempe,[4] Jared Tracy,[5] Kausik R. Choudhury,[5] William J. Gambogi,[5] Laura S. Bruckman,[1] and Kenneth P. Boyce[3]

1 Case Western Reserve University
2 National Insitute of Standards and Technology
3 Underwriter Laboratories
4 National Renewable Energy Laboratory
5 DuPont Photovoltaic Solutions
6 Arkema, King of Prussia

Suggested Citation
Wieser. Raymond J., et al. 2022. *Spatiotemporal Modeling of Real World Backsheets Field Survey Data: Hierarchical (Multilevel) Generalized Additive Models: Preprint*. Golden, CO: National Renewable Energy Laboratory. NREL/CP-5K00-81961. https://www.nrel.gov/docs/fy22osti/81961.pdf.

NREL is a national laboratory of the U.S. Department of Energy
Office of Energy Efficiency & Renewable Energy
Operated by the Alliance for Sustainable Energy, LLC

This report is available at no cost from the National Renewable Energy Laboratory (NREL) at www.nrel.gov/publications.

Contract No. DE-AC36-08GO28308

Conference Paper
NREL/CP-5K00-81961
September 2022

National Renewable Energy Laboratory
15013 Denver West Parkway
Golden, CO 80401
303-275-3000 • www.nrel.gov

NOTICE

This work was authored in part by the National Renewable Energy Laboratory, operated by Alliance for Sustainable Energy, LLC, for the U.S. Department of Energy (DOE) under Contract No. DE-AC36-08GO28308. Funding provided by the U.S. Department of Energy Office of Energy Efficiency and Renewable Energy under Solar Energy Technologies Office (SETO) Agreement Number DEEE-0008748. The views expressed herein do not necessarily represent the views of the DOE or the U.S. Government. The U.S. Government retains and the publisher, by accepting the article for publication, acknowledges that the U.S. Government retains a nonexclusive, paid-up, irrevocable, worldwide license to publish or reproduce the published form of this work, or allow others to do so, for U.S. Government purposes.

This report is available at no cost from the National Renewable Energy Laboratory (NREL) at www.nrel.gov/publications.

U.S. Department of Energy (DOE) reports produced after 1991 and a growing number of pre-1991 documents are available free via www.OSTI.gov.

Cover Photos by Dennis Schroeder: (clockwise, left to right) NREL 51934, NREL 45897, NREL 42160, NREL 45891, NREL 48097, NREL 46526.

NREL prints on paper that contains recycled content.

Spatiotemporal Modeling of Real World Backsheets Field Survey Data: Hierarchical (Multilevel) Generalized Additive Models

Raymond J. Wieser*, Zelin(Zack) Li*, Stephanie L. Moffitt†, Ruben Zabalza‡, Evan Boucher‡, Silvana Ayala§, Matthew Brown§, Xiaohong Gu†, Liang Ji‡, Colleen O'Brien‡, Adam W. Hauser‖, Greg S. O'Brien‖, Xuanji Yu*, Roger H. French*, Micheal D. Kempe§, Jared Tracy¶, Kausik R. Choudhury¶, William J. Gambogi¶, Laura S. Bruckman* , Kenneth P. Boyce‡

* Case Western Reserve University, Cleveland, Ohio, 44106, USA

† National Insitute of Standards and Technology, Gaithersburg, Maryland, 20878, USA

‡ Underwriter Laboratories, Northbrook, Illinois, 60062, USA

§ National Renewable Energy Laboratory, Golden, Colorado, 80401, USA

¶ DuPont Photovoltaic Solutions, Wilmington DE, 19803, USA

‖ Arkema, King of Prussia, Pennsylvania, 19406, USA

***Abstract*—Assessing photovoltaic module backsheet durability is critical to increasing module lifetime. Laboratory-based accelerating testing has recently failed to predict large scale failures of widely adopted polymeric materials. Additionally, there is a growing concern on characterizing the non-uniformity of field exposure. Therefore, data from field surveys are critical to assess the performance of component lifetimes. Using a documented field survey protocol, 19 field surveys were conducted. The focus of this survey strategy is to investigate spatial continuity in degradation modes. By combining field survey data with real-time satellite weather data, stressor / response models have been trained. Generalized additive Models (GAM) model was created to predict the value of degradation based on measured predictors. Two different GAM constructions were testing using different implementations of basis splines. The model includes variables on the environmental stressors of the system and the location of each measurement in the PV mounting structure. The incorporation of hierarchical structure into the models allowed for material specific degradation rates, while maintaining the assumption of a global trend. The model performed well with an adjusted R^2 of 0.975 for yellowness index prediction.**

***Index Terms*—Backsheet, Degradation, Spatio-temporal, Modeling, Field Survey,**

I. Introduction

To be cost effective, utility-scale power providers are reliant on Photovoltaic (PV) module service lifetimes exceeding 20 years of operation in a variety of exposure environments. PV backsheets are affected by multiple environmental stressors and degrade due to synergistic effects in the field. The study of outdoor backsheets degradation is necessary to understand real-world PV failure and improve accelerated testing protocols. However, current research on outdoor backsheet degradation is much scarcer than that of PV cells or encapsulants [1], [2].

Backsheets in installed PV modules experience various synergistic stressors, including irradiance, temperature, humidity, abrasion, and other factors. Ultraviolet (UV) light reflected from the ground can cause chain scission and loss of mechanical strength [3], [4]. The diurnal and seasonal thermal cycles create thermal-mechanical stress, contributing to backsheet failures [5]. The presence of moisture can also have dramatic effects on the degradation of backsheet materials [6]–[11]. These stressors also vary spatially according to array geometry, changes in ground albedo, and shading due to external objects. It was found that the edge modules experienced higher degradation rates, attributed to an increase of rear-side irradiance [12], [13].

Field survey data has recently been used to illuminate effects observed in long-term outdoor exposures. Measurements of the color and gloss of PV modules after years of outdoor exposure showed differential degradation patterns based on the PV mounting structure [1]. Additionally, this observed trend was modeled using generalized additive modeling (GAM), resulting in an equation that predicted degradation patterns across the surface of the PV backsheet based on its location in the mounting structure [13]. It was found that the edges of PV mounting systems experience faster rates of apparent degradation than the modules located at the center. Moreover, it was found that the distance from the ground was another factor in the degradation rate. An improved GAM was developed using data from 14 individual field surveys. However,

This material is based upon work supported by the U.S. Department of Energy's Office of Energy Efficiency and Renewable Energy (EERE) under Solar Energy Technologies Office (SETO) Agreement Number DE-EE-0008748. The views expressed herein do not necessarily represent the views of the U.S. Department of Energy or the United States Government. This work made use of the Rider High Performance Computing Resource in the Core Facility for Advanced Research Computing at Case Western Reserve University.

the model struggled to differentiate the synergistic effects of climate stressors [14].

This study improves on past GAM modeling efforts with a new hierarchical modeling framework, which allows for pooled model coefficients. Hierarchical (Multilevel / Mixed Effect) modeling has widely been used to model spatio-temporal data in the fields of ecology, finanace, and real-estate [15] [16] [17] [18] [19]. To better parse out the synergistic effects of multiple climatic stressors, a field survey was conducted where multiple backsheet brands and materials were exposed under the same environment. This survey will allow a comparison of the material-specific degradation modes that are excited by the same levels of environmental stressors.

II. Methodology

A. Field Survey Protocol

A field survey protocol was defined to standardize the measurement locations and the measurement types recorded to produce a uniform data set. This protocol has been applied to 19 PV systems. The current protocol dictates that individual rows of PV modules will be measured systematically, with uniform separation of measurements along the length of the row. It is recommended that a minimum of 12 modules should be recorded for each row measured, but for long rows, the number of modules should increase. Additionally, to observe the 'edge effect', additional modules are surveyed on the row ends. Each module is measured in 6 locations across the surface of its backsheet. Data is collected on the Yellowness Index (ATSM E313), Gloss (ASTM D523), and FTIR spectra of every module surveyed without cleaning the module. The exposure conditions of the field are also noted.

This study presents measurements of four different types of air-side backsheet materials. Polyvinylidene diflouride (PVDF), and Polyvinyl Fluoride (PVF) are fluoro-polymer based films. Fluoroethylene vinyl ether (FEVE) is a spray type fluoro-polymer coating applied to backsheet films. Polyethylene naphthalate (PEN) is a non-fluoropolymer film.

B. Data

Weather data for PV sites was gathered using SolarGIS. The data consisted of temperature, relative humidity, global horizontal irradiance, diffuse horizontal irradiance, and wind speed. Measurements were recorded at five-minute intervals for up to four years. The climate data was obtained from the closest available weather station and ingested into a high performance computer. When available, weather data collected at the specific PV installation is used.

After conducting a field survey, the instrument data is processed through cleaning scripts that label and supplement each observation with meta-data. After the data is cleaned, it is ingested into Case Western's High-Performance Computing Cluster and stored.

C. Modeling

1) Inference By Eye: Inference by Eye is a statistical technique developed to quickly visualize and test for the statistical significance at the 0.05 level, of both null hypothesis testing and two sample t-tests [20]–[22]. With a 95% confidence interval (CI), it can be used to test if a module has undergone a change over time, such that the null hypothesis test fails and the sample has undergone significant change at a 0.05 significance level. And it can be used to compare among many samples, using a two sample t-test and 83.5% CIs, that two samples significantly different from each other at the 0.05 significance level. The basic principle of this technique relies on a simple 2-sample independent students t-test of the difference between two means ($p = 0.05$, $t = 1.96$). A more in-depth discussion of inference by eye can be found in the following paper by Wieser et al. [14].

2) Generalized Additive Modeling: To predict the values of degradation, GAMs have been created to relate the observed responses to real world stressors on the field survey data. Smoothing splines have been integrated as the basis functions for the spatial variability of the observed data. More information on the principles of applying GAM to field survey data can be found in Wieser et al. [14].

The hierarchical extension of a GAM allows for group-specific variations in the overall trend of the model. Hierarchical models allow for flexibility in the fit parameters based on the structure of the data. In particular, the hierarchical model allows for different coefficients for each of the material types in the study while maintaining the assumption that all the observed responses have a shared global trend.

Two approaches to GAM modeling will be discussed. The first approach uses the natural spline model as a regressor in the GAM model (Equation 1), whereas the other approach incorporates and penalizes the spline fitting into the model (Equation 2). In other words, the first approach takes an existing predetermined spline function based off of the co-variate as a variable in the model. The second approach models and minimizes the variance in spline terms while determining the coefficients for each term. The advantage of the second model structure is its ability to capture the hierarchical differences in the structure of the field data. The individual smoothing splines are created as an ensemble of functions that can be penalized through different constraints. For the purposes of this analysis, each material will be considered its own group, and the model will allow for individual smoothing parameters for each material. This results in a model that acknowledges a global shared trend for the spatial dependence of material degradation, but allows material specific flexibility to account for differential rates of degradation.

Along with the information gathered from the field surveys, weather data is also being incorporated into the GAM model. Years' worth of time-series weather data are aggregated, generating general statistics on the climate of each location.

The spatio model of degradation contains variables for the position of the module in the row structure, Length (**L**) and Depth (**D**) and interaction between material (M_i) and exposure condition (E_j). The model change point locations a_1 and a_2 determine the position of the knots in the regression form of the GAM. The temporal model includes the following parameters: time of contact wetness (**CW**), cumulative yearly irradiance (**IRR**), time at elevated temperature (**TAET**), and time (**t**).

The general form of the spatio- equation then can be expressed as:

$$Y(L,D,M) = \beta_0 + \beta_1 L + \beta_2 L^2 + \beta_3 L^3 + \beta_4 (L - a_1) + \beta_5 (L - a_2) + \beta_6 D + \beta_7 D^2 + \beta_{M,E} \quad (1)$$

or

$$Y(L,D,M) = \beta_0 + f(L) + f(D) + \beta_{M,E} \quad (2)$$

where $f(L)$ and $f(D)$ are spline terms defined as in Equation 3.

$$f(X) = \sum_{q=0}^{Q} \beta_q \cdot b_q(X) = \beta_0 + \beta_1 b_1(X) + \beta_2 b_2(X) + \ldots + \beta_Q b_Q(X) \quad (3)$$

With the general form of the temporal equation:

$$Y(CW, IRR, TAET, t) = \beta_1(CW \times t) + \beta_2(IRR \times t) + \beta_3(TAET \times t) + \beta_4(M_i \times t) \quad (4)$$

The GAM creates all the components separately using a linear combination of all the unique equations for each variable.

Model validation was conducted using the Akaike Information Criterion (AIC), which allows the comparison of GAMs with different combinations of effects. The models were built on subsetted data-sets with 80% of the data allocated to the training of the model. Root Mean Squared Estimates (RMSE) and Adj. R^2 values were used to evaluate the model fit. Two baseline models (linear and piece-wise) were developed to evaluate the performance of the GAMs.

III. Results / Discussion

A. Spatial Modeling

GAMs were created using both approaches. The overall fit of both models provided additional insight into the spatial dependence of degradation. However, the natural spline regression GAM struggled to capture the different mechanisms of degradation. Fluoropolymer based materials are shown to degrade to values of negative YI, whereas other backsheet materials tend to increase their YI. The natural spline model does not differentiate between these mechanisms, and fits the edges of the spatial function to be concave down (becoming more negative), due to the presence of fluoropolymers. However, the penalized smoothing GAM intrinsically captures group specific effects and allows for different functional responses. This allows the penalized smoothing GAM to differentiate between materials that have different degradation responses.

TABLE I: Approximate Significance of the Penalized Splines

Term	Material	Est. Deg. of Freedom	Ref. Deg. of Freedom	Statistic	P-Value
$f(L)$	PVF	0.0002484	36	0.0000016	0.7527733
$f(L)$	FEVE	0.8294896	39	0.0665848	0.0472572
$f(L)$	PEN	22.9198381	26	7.9638536	<2 E -16
$f(L)$	PVDF	1.0228291	39	0.0493353	0.1271306
$f(D)$	PVF	2.2568605	8	0.5338434	0.0999844
$f(D)$	FEVE	0.0114537	7	0.0030046	<2 E -16
$f(D)$	PEN	3.0013728	6	5.6328328	<2 E -16
$f(D)$	PVDF	0.9892293	7	0.2419582	0.0076261

Therefore, the penalized smoothing GAM was able to better model the spatial component of the degradation response (Figure 2). However, there are certain cases where the penalization of the smoothing splines resulted in the loss of information of high frequency spatial dependence. While the penalized smoothing splines fit the overall shape of the data, the natural spline's knots allowed for increased flexibility to capture more of the spatial variance of the observed signal (Figure 1). The resultant smoothing splines from the penalized GAM model can be used to investigate material specific spatial trends. It was shown that the different materials exhibit varying degrees of spatial dependence. The polymers PEN and FEVE where shown to have a strong spatial dependence, where as the fluoro-polymer films did not have a significant dependence on the spatial location of measurement (Table I). A lack of spatial dependence indicates that the material is less sensitive to micro-climatic effects.

The location of the row in the overall field was also analyzed to determine if the row location had a significant effect on the level of degradation observed. The models include separate intercept terms for the different combinations of material type and row exposure conditions. The row exposure of "Fully Shaded" was used as the base case for the model. Interaction terms without data where excluded from the table. Both GAM models found significant effects in the interaction between row exposure and material type. PEN and PVF based backsheets showed varying levels of degradation for different row locations. Frontside unshaded rows exhibited less severe levels of degradation compared to the fully shaded rows.

B. Temporal Modeling

The spatial component of the GAMs captures the anisotropic degradation of backsheet materials. This allows the temporal components to be modeled by removing the variance due to the differences in local exposure conditions. The temporal coefficients can be divided into climatic stressors and material aging effects.

Both GAMs found significant contributions between the interaction terms of climatic stressor and length of exposure (Table III). The annual total dose of irradiance is the strongest contributor to the observed degradation. The other climatic stressor terms had smaller contributions to the overall level of degradation observed. The presence of dew formation and exposure to elevated temperature (T $<35°$C) were found to

TABLE II: Significance of interaction between row exposure environment and material type, as compared to the base case of "Fully Shaded"

Model	Term	Material	Row Environment	Estimate	Std. Error	t value	P-Value
Natural Spline GAM	$\beta_{M,E}$	PVF	Frontside Unshaded	1.314e+00	1.181e-01	11.124	<2e-16
	$\beta_{M,E}$	FEVE	Frontside Unshaded	-2.959e-02	1.717e-01	-0.250	0.803
	$\beta_{M,E}$	PEN	Frontside Unshaded	-5.272e-01	1.238e-01	-4.285	1.87e-05
	$\beta_{M,E}$	PVDF	Frontside Unshaded	-4.897e-02	8.992e-02	0.247	0.805
	$\beta_{M,E}$	FEVE	Rearside Unshaded	9.443e-02	1.716e-01	0.507	0.612
	$\beta_{M,E}$	PEN	Rearside Unshaded	-2.124e+00	1.568e-01	-13.551	<2e-16
	$\beta_{M,E}$	PVDF	Rearside Unshaded	-1.367e-01	8.933e-02	-0.712	0.476
	$\beta_{M,E}$	PVF	Tracker	-1.364e+00	1.177e-01	-11.581	<2e-16
Penalized Smooth GAM	$\beta_{M,E}$	PVF	Frontside Unshaded	1.088e+00	6.354e-02	17.123	<2e-16
	$\beta_{M,E}$	FEVE	Frontside Unshaded	-2.862e-02	1.397e-01	-0.231	0.817439
	$\beta_{M,E}$	PEN	Frontside Unshaded	-4.043e-01	1.057e-01	-3.823	0.000134
	$\beta_{M,E}$	PVDF	Frontside Unshaded	1.486e-02	7.316e-02	0.308	0.757991
	$\beta_{M,E}$	FEVE	Rearside Unshaded	8.903e-02	1.397e-01	0.644	0.519766
	$\beta_{M,E}$	PEN	Rearside Unshaded	-5.405e-01	1.578e-01	-3.430	0.000610
	$\beta_{M,E}$	PVDF	Rearside Unshaded	-4.385e-02	7.259e-02	-0.476	0.633842
	$\beta_{M,E}$	PVF	Tracker	-1.136e+00	6.305e-02	-18.055	<2e-16

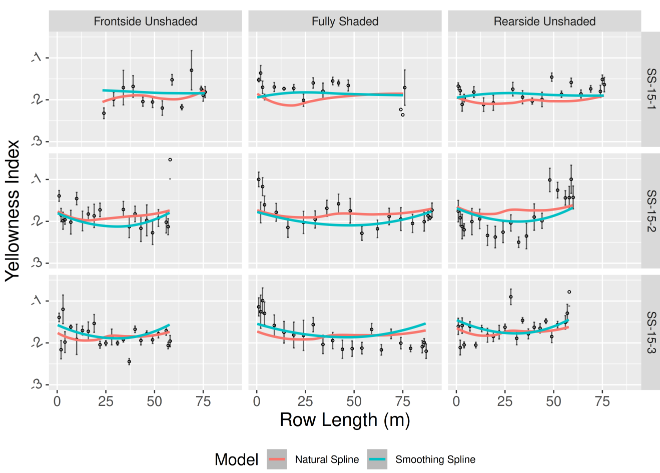

Fig. 1: Results of predicting the trained model on the SS-15 Sites. This model was fitted using an 80% training set.

TABLE III: Interaction terms between length of exposure and climatic stressor.

Model	Term	Stressor	Estimate	Std. Error	T-Value	P-Value
NS GAM	β_1	CW	-3.798e-03	6.938e-04	-5.475	4.65e-08
	β_2	IRR	1.714e-06	9.941e-08	17.241	<2e-16
	β_3	TAET	-4.787e-04	7.794e-05	-6.143	8.92e-10
PS GAM	β_1	CW	-8.479e-03	4.882e-04	-17.367	<2e-16
	β_2	IRR	2.309e-06	7.099e-08	32.525	<2e-16
	β_3	TAET	-8.563e-04	5.565e-05	-15.388	<2e-16

decrease the observed values of degradation. This could relate to the formation of differently colored degradation products. However, the observed effects could be the result of the GAM overfitting some of the variance of the material degradation behaviors.

Material specific degradation rates were also modeled using

TABLE IV: Interaction terms between length of exposure and material type. These values can be used to determine the types of degradation products formed and susceptibility of the material to exposure.

Model	Term	Material	Estimate	Std. Error	t-Value	P-Value
NS GAM	β_4	PVF	-4.939e-01	1.867e-02	-26.454	<2e-16
	β_4	FEVE	-8.597e-01	4.738e-02	-18.147	<2e-16
	β_4	PEN	2.023e+00	2.338e-02	86.523	<2e-16
	β_4	PVDF	-5.599e-01	4.119e-02	-13.592	<2e-16
PS GAM	β_4	PVF	-4.738e-01	2.683e-02	-17.656	<2e-16
	β_4	FEVE	-6.791e-01	6.710e-02	-10.120	<2e-16
	β_4	PEN	2.216e+00	3.199e-02	69.266	<2e-16
	β_4	PVDF	-7.864e-01	3.428e-02	-22.938	<2e-16

the temporal equation. Over the length of the exposure the fluoro-polymer based materials tend to decrease in the value of YI (turning blue). This observed response to exposure is well captured by both GAMs. The magnitude of these coefficients also provides information on the susceptibility of a material to the formation of degradation products. The fluoro-polymer based backsheets have low coefficients which is related to their overall stability under outdoor exposure. PEN based backsheets exhibited the highest rates of the formation of degradation products IV.

C. *Model Fit*

Overall the models fit the highly variable data well. The spline terms were able to capture some of the spatial variability in the data. The penalized smoothing spline exhibited lower RMSE and higher adj.R^2. The increase of flexibility of the penalized smoothing model allowed for a better model of the spatial variance of the data. There was little difference between the RMSE values of the testing and training data-sets for both models, indicating that they did not over-fit the training data-set. Although not discussed, a simple linear model and a piece-wise model were used as baseline models. The model accuracy parameters can be found in Table V.

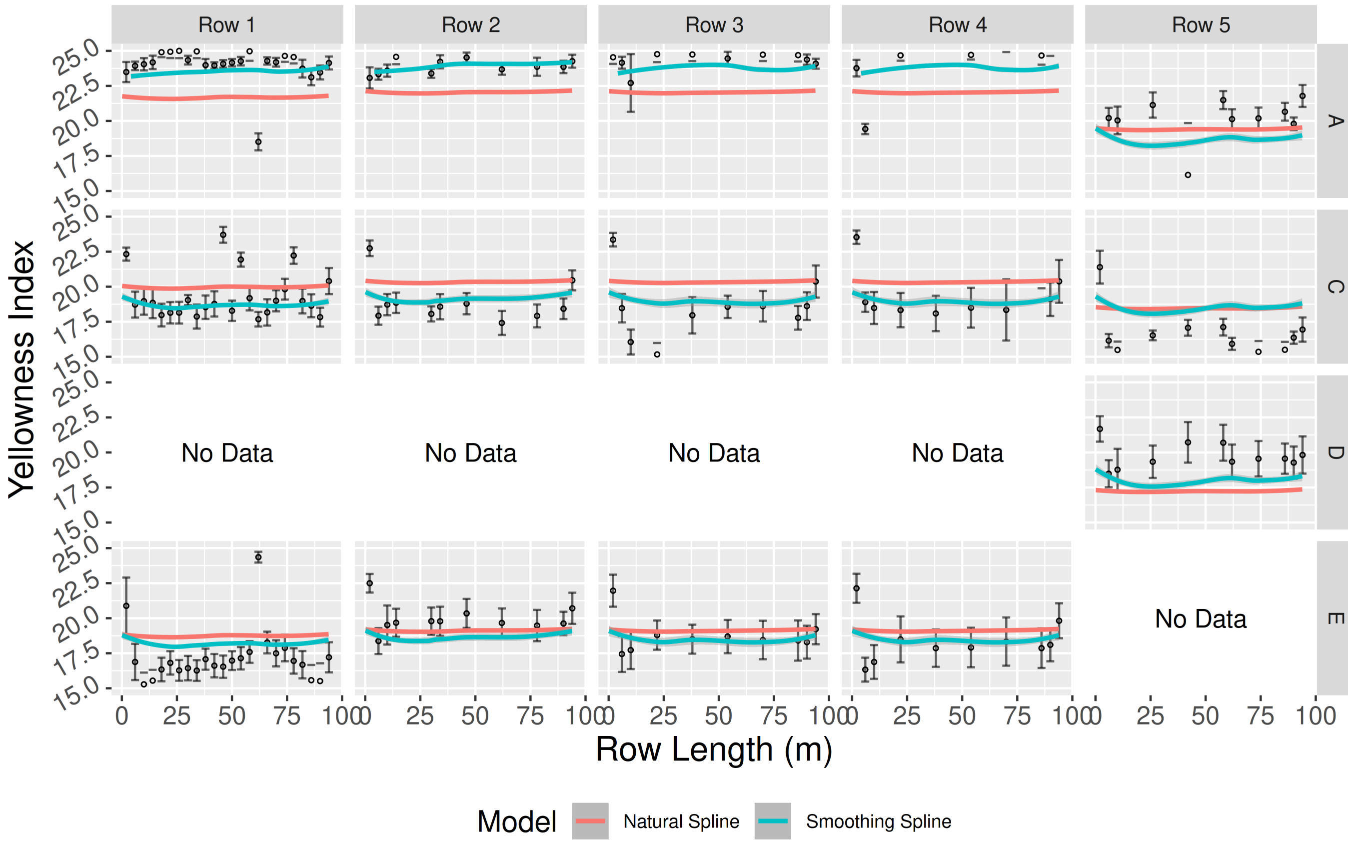

Fig. 2: Results of predicting the trained model on the SS-16-1 Site. This model was fitted using a 80% training set.

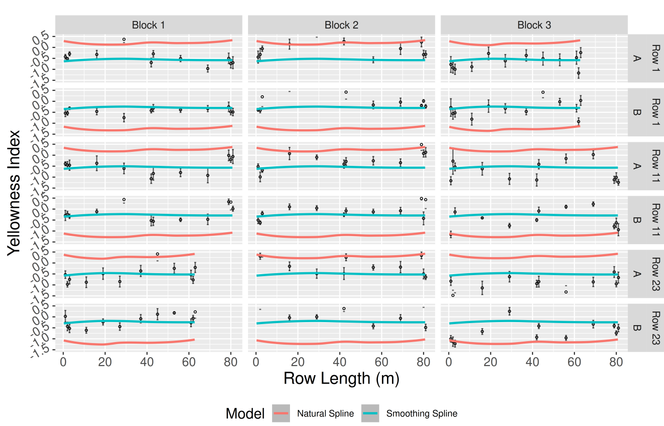

Fig. 3: Results of predicting the trained model on the SS-16-2 Site. This model was fitted using a 80% training set.

TABLE V: Model Accuracy Parameters

Model	$adj R^2$	RMSE Training	RMSE Testing
Linear Model	0.834	2.35	3.35
Piecewise Model	0.883	2.12	2.34
Natural Spline	0.962	1.675	1.626
Penalized Smoothing	0.975	1.339	1.355

IV. Conclusions

GAMs present a highly flexible framework to analyze hierarchically structure problems. Through careful survey design, a multitude of different exposure related degradation modes can be quantified. Interaction terms between length of exposure and climatic stressor allow for a deeper understanding of the pertinent climatic variables that affect material longevity. In addition, the stability of materials during outdoor exposure can be directly compared. The sensitivity to changes in microclimatic exposure can be understood through the contribution of smoothing splines. It was found that the fluoro-polymer based backsheets were the least susceptible to degradation and the least sensitive to changes in environment.

References

[1] A. Fairbrother, M. Boyd, Y. Lyu, J. Avenet, P. Illich, Y. Wang, M. Kempe, B. Dougherty, L. Bruckman, and X. Gu, “Differential degradation patterns of photovoltaic backsheets at the array level,” *Solar Energy*, vol. 163, pp. 62–69, Mar. 2018.

[2] W. Gambogi, Y. Heta, K. Hashimoto, J. Kopchick, T. Felder, S. MacMaster, A. Bradley, B. Hamzavytehrany, L. Garreau-Iles, T. Aoki, K. Stika, T. J. Trout, and T. Sample, “A Comparison of Key PV Backsheet and Module Performance from Fielded Module Exposures and Accelerated Tests,” *IEEE Journal of Photovoltaics*, vol. 4, no. 3, pp. 935–941, May 2014.

[3] Y. Lyu, J. H. Kim, A. Fairbrother, and X. Gu, "Degradation and Cracking Behavior of Polyamide-Based Backsheet Subjected to Sequential Fragmentation Test," *IEEE Journal of Photovoltaics*, pp. 1–6, 2018.

[4] C.-C. Lin, Y. Lyu, L.-C. Yu, and X. Gu, "Correlation between mechanical and chemical degradation after outdoor and accelerated laboratory aging for multilayer photovoltaic backsheets," in *Reliability of Photovoltaic Cells, Modules, Components, and Systems IX*, vol. 9938. International Society for Optics and Photonics, Sep. 2016, p. 99380H. [Online]. Available: https://doi.org/10.1117/12.2238216

[5] A. Omazic, G. Oreski, M. Halwachs, G. C. Eder, C. Hirschl, L. Neumaier, G. Pinter, and M. Erceg, "Relation between degradation of polymeric components in crystalline silicon PV module and climatic conditions: A literature review," *Solar Energy Materials and Solar Cells*, vol. 192, pp. 123–133, Apr. 2019, citation Key Alias: omazicRelationDegradationPolymeric2019a. [Online]. Available: http://www.sciencedirect.com/science/article/pii/S0927024818305956

[6] International Electrotechnical Commission, "IEC 61215 Terrestrial photovoltaic (PV) modules - Design qualification and type approval," International Electrotechnical Commission, International Standard, 2016. [Online]. Available: https://webstore.iec.ch/publication/24312

[7] M. D. Kempe and J. H. Wohlgemuth, "Evaluation of temperature and humidity on PV module component degradation," in *2013 IEEE 39th Photovoltaic Specialists Conference (PVSC)*, Jun. 2013, pp. 0120–0125.

[8] E. Wang, H. E. Yang, J. Yen, S. Chi, and C. Wang, "Failure Modes Evaluation of PV Module via Materials Degradation Approach," *Energy Procedia*, vol. 33, pp. 256–264, Jan. 2013. [Online]. Available: http://www.sciencedirect.com/science/article/pii/S1876610213000763

[9] N. Kim, H. Kang, K.-J. Hwang, C. Han, W. S. Hong, D. Kim, E. Lyu, and H. Kim, "Study on the degradation of different types of backsheets used in PV module under accelerated conditions," *Solar Energy Materials and Solar Cells*, vol. 120, pp. 543–548, Jan. 2014. [Online]. Available: https://doi.org/10.1016/j.solmat.2013.09.036

[10] W. Gambogi, Y. Heta, K. Hashimoto, J. Kopchick, T. Felder, S. MacMaster, A. Bradley, B. Hamzavytehraney, V. Felix, T. Aoki, K. Stika, L. Garreau-Illes, and T. J. Trout, "Weathering and durability of PV backsheets and impact on PV module performance," in *Reliability of Photovoltaic Cells, Modules, Components, and Systems VI*, vol. 8825. International Society for Optics and Photonics, Sep. 2013, p. 88250B. [Online]. Available: https://www.spiedigitallibrary.org/conference-proceedings-of-spie/8825/88250B/Weathering-and-durability-of-PV-backsheets-and-impact-on-PV/10.1117/12.2024491.short

[11] F. Liu, L. Jiang, and S. Yang, "Ultra-violet degradation behavior of polymeric backsheets for photovoltaic modules," *Solar Energy*, vol. 108, pp. 88–100, Oct. 2014. [Online]. Available: http://www.sciencedirect.com/science/article/pii/S0038092X14003260

[12] A. Fairbrother, M. Boyd, Y. Lyu, J. Avenet, P. Illich, Y. Wang, M. Kempe, B. Dougherty, L. Bruckman, and X. Gu, "Differential degradation patterns of photovoltaic backsheets at the array level," *Solar Energy*, vol. 163, Feb. 2018. [Online]. Available: https://doi.org/10.1016/j.solener.2018.01.072

[13] Y. Wang, W.-H. Huang, A. Fairbrother, L. S. Fridman, A. J. Curran, N. R. Wheeler, S. Napoli, A. W. Hauser, S. Julien, X. Gu, G. S. O'Brien, K.-T. Wan, L. Ji, M. D. Kempe, K. P. Boyce, R. H. French, and L. S. Bruckman, "Generalized Spatio-Temporal Model of Backsheet Degradation From Field Surveys of Photovoltaic Modules," *IEEE Journal of Photovoltaics*, vol. 9, no. 5, pp. 1374–1381, Sep. 2019.

[14] R. J. Wieser, K. Rath, S. L. Moffitt, R. Zabalza, E. Boucher, S. Ayala, M. Brown, X. Gu, L. Ji, C. O'Brien, A. W. Hauser, G. S. O'Brien, R. H. French, M. D. Kempe, J. Tracy, K. R. Choudhury, W. J. Gambogi, L. S. Bruckman, and K. P. Boyce, "Spatio-Temporal Modeling of Field Surveyed Backsheet Degradation," in *2021 IEEE 48th Photovoltaic Specialists Conference (PVSC)*, Jun. 2021, pp. 1383–1388, iSSN: 0160-8371.

[15] J. M. Diez and H. R. Pulliam, "Hierarchical Analysis of Species Distributions and Abundance Across Environmental Gradients," *Ecology*, vol. 88, no. 12, pp. 3144–3152, 2007, _eprint: https://onlinelibrary.wiley.com/doi/pdf/10.1890/07-0047.1. [Online]. Available: https://onlinelibrary.wiley.com/doi/abs/10.1890/07-0047.1

[16] S. M. McMahon and J. M. Diez, "Scales of association: hierarchical linear models and the measurement of ecological systems," *Ecology Letters*, vol. 10, no. 6, pp. 437–452, 2007, _eprint: https://onlinelibrary.wiley.com/doi/pdf/10.1111/j.1461-0248.2007.01036.x. [Online]. Available: https://onlinelibrary.wiley.com/doi/abs/10.1111/j.1461-0248.2007.01036.x

[17] R. A. Chisholm, H. C. Muller-Landau, K. Abdul Rahman, D. P. Bebber, Y. Bin, S. A. Bohlman, N. A. Bourg, J. Brinks, S. Bunyavejchewin, N. Butt, H. Cao, M. Cao, D. Cárdenas, L.-W. Chang, J.-M. Chiang, G. Chuyong, R. Condit, H. S. Dattaraja, S. Davies, A. Duque, C. Fletcher, N. Gunatilleke, S. Gunatilleke, Z. Hao, R. D. Harrison, R. Howe, C.-F. Hsieh, S. P. Hubbell, A. Itoh, D. Kenfack, S. Kiratiprayoon, A. J. Larson, J. Lian, D. Lin, H. Liu, J. A. Lutz, K. Ma, Y. Malhi, S. McMahon, W. McShea, M. Meegaskumbura, S. Mohd. Razman, M. D. Morecroft, C. J. Nytch, A. Oliveira, G. G. Parker, S. Pulla, R. Punchi-Manage, H. Romero-Saltos, W. Sang, J. Schurman, S.-H. Su, R. Sukumar, I.-F. Sun, H. S. Suresh, S. Tan, D. Thomas, S. Thomas, J. Thompson, R. Valencia, A. Wolf, S. Yap, W. Ye, Z. Yuan, and J. K. Zimmerman, "Scale-dependent relationships between tree species richness and ecosystem function in forests," *Journal of Ecology*, vol. 101, no. 5, pp. 1214–1224, 2013, _eprint: https://onlinelibrary.wiley.com/doi/pdf/10.1111/1365-2745.12132. [Online]. Available: https://onlinelibrary.wiley.com/doi/abs/10.1111/1365-2745.12132

[18] J. D. McCabe, J. D. Clare, T. A. Miller, T. E. Katzner, J. Cooper, S. Somershoe, D. Hanni, C. A. Kelly, R. Sargent, E. C. Soehren, C. Threadgill, M. Maddox, J. Stober, M. Martell, T. Salo, A. Berry, M. J. Lanzone, M. A. Braham, and C. J. W. McClure, "Resource selection functions based on hierarchical generalized additive models provide new insights into individual animal variation and species distributions," *Ecography*, vol. n/a, no. n/a, _eprint: https://onlinelibrary.wiley.com/doi/pdf/10.1111/ecog.06058. [Online]. Available: https://onlinelibrary.wiley.com/doi/abs/10.1111/ecog.06058

[19] E. J. Pedersen, D. L. Miller, G. L. Simpson, and N. Ross, "Hierarchical generalized additive models in ecology: an introduction with mgcv," *PeerJ*, vol. 7, p. e6876, 2019.

[20] G. Cumming and S. Finch, "Inference by Eye: Confidence Intervals and How to Read Pictures of Data," *American Psychologist*, vol. 60, no. 2, pp. 170–180, 2005, place: US Publisher: American Psychological Association.

[21] A. Hazra, "Using the confidence interval confidently," *Journal of Thoracic Disease*, vol. 9, no. 10, pp. 4124–4129, Oct. 2017, tex.ids= hazraUsingConfidenceInterval2017 publisher: AME Publishing Company. [Online]. Available: http://jtd.amegroups.com/article/view/16406/13455

[22] J. Leppink, "A Pragmatic Approach to Statistical Testing and Estimation (PASTE)," *Health Professions Education*, vol. 4, no. 4, pp. 329–339, Dec. 2018. [Online]. Available: https://www.sciencedirect.com/science/article/pii/S2452301117301487